Two-class freeway traffic regulation to reduce congestion and emissions via nonlinear optimal control

Cecilia Pasquale[b], Ioannis Papamichail[a], Claudio Roncoli[a],
Simona Sacone[b], Silvia Siri[b], Markos Papageorgiou[a]

[a] *Dynamic Systems and Simulation Laboratory,*
Technical University of Crete, Greece
[b] *Department of Informatics, Bioengineering, Robotics and Systems Engineering,*
University of Genova, Italy

Abstract

The objective of this paper is the regulation of freeway traffic by means of optimal control techniques. A first innovative aspect of the proposed approach is the adopted objective function in which, besides the reduction of traffic congestion (which is typically considered in traffic control schemes), the minimization of traffic emissions is also included. Moreover, a multi-class framework is defined in which two classes of vehicles (cars and trucks) are explicitly modelled, and specific control actions for each vehicle class are sought. This results in the formulation of a multi-objective optimal control problem which is described in the paper and for which a specific solution algorithm is developed and used. The algorithm exploits a specific version of the feasible direction algorithm whose effectiveness is demonstrated in the paper by means of simulation results.

Keywords: Freeway traffic control, two-class traffic model and control, ramp metering, traffic emissions

1. Introduction

Phenomena of recurrent and nonrecurrent congestion in freeway systems can be relieved by applying proper control techniques, that have been studied by researchers for some decades. A very successful and widespread control measure is ramp metering, which allows to control the traffic flow entering the freeway mainstream by using traffic lights at the on-ramps. Ramp metering is applied to achieve maximum mainline throughput downstream

of the ramp (local control) or, more generally, optimal traffic conditions in the freeway network (networkwide approaches) [1]. One of the first effective ramp metering strategies is the local feedback traffic controller ALINEA [2], dating back to the Nineties, that has been applied in many freeways all over the world. It has been shown that ALINEA, despite being a local controller, is quite effective in increasing the motorway throughput [3]. During the years, ALINEA has been further extended, resulting in a proportional-integral version, called PI-ALINEA [4], or through a coordination of the local ramp-metering actions, thus enabling the linked control of the inflow from consecutive on-ramps [5].

Different traffic control methodologies have been developed in the last decades, also including approaches based on optimization or optimal control algorithms [6]. In some works, the problem of controlling a freeway is formulated as a discrete-time constrained nonlinear optimal control problem (see [7] and the references therein), whose numerical solution is often hard to find by directly using the available Nonlinear Programming codes, because of the problem dimensions and complexity. A very efficient numerical solution has been adopted in the optimal freeway traffic control tool AMOC [8, 9], by using the so-called feasible direction algorithm. Then, more sophisticated control architectures have been investigated, again based on AMOC, such as for instance the three-layer hierarchical control approach described in [10] and the mainstream traffic flow control scheme proposed in [11].

Optimal control algorithms may be embedded in Model Predictive Control schemes, using real-time measurements (feedback) as initial states. For instance, in [12, 13] nonlinear MPC frameworks adopting the macroscopic model METANET [14] for prediction are presented and described. Also in these works, nonlinear optimization problems have to be solved, since the considered prediction model is nonlinear, thus efficient numerical solution algorithms are needed to enable on-line application for large freeway networks. In other approaches, e.g. [15, 16, 17], the considered prediction models are rewritten in linear form by adding integer and binary variables to the finite horizon optimal control problem, which turns out to have a mixed-integer linear or quadratic programming form.

In most of the research works dealing with ramp metering control the main objective of the controller is to minimize congestion, often measured in terms of total time spent by the drivers in the traffic network [18]. However, the congestion reduction is not the only important objective to pursue, since there are other aspects to be considered in traffic control schemes, such

as the minimization of traffic emissions. For instance, in [19] a control approach to minimize both travel times and traffic emissions on freeways is discussed, while [20] presents a dynamic model for the dispersion of freeway traffic emissions. Moreover, [21] proposes a parameterized MPC approach where the travel times and the traffic emissions are minimized jointly, and in [22] an MPC scheme is considered in which the macroscopic traffic flow models and the microscopic emission and fuel consumption models are properly integrated.

In order to explicitly consider traffic emissions as an objective to be minimized, models for evaluating hot exhaust emissions are needed. Emission models have been studied for some decades [23] and can be classified according to the geographical scale, the accuracy of the model, and the nature of the emission calculation approach. Among others, simple but very widespread models are the so-called average-speed emission models which assume that the average emission factor for a certain pollutant and a given type of vehicle only depends on the average speed during a trip [24]. Different average-speed models have been studied and progressively updated including new vehicle classifications and new emission factors, on the basis of real measured data obtained from different sources [25, 26].

In this paper, we propose a freeway traffic control approach which considers, as control objectives, both the minimization of traffic emissions and the reduction of traffic congestion. A similar idea was proposed in previous works [27, 28], where the control scheme was based on a local regulator inspired by ALINEA. In this work, instead, an optimal control problem is formulated and solved by applying the feasible direction algorithm and, in particular, a specific version of this algorithm which adopts the derivative backpropagation method RPROP, the effectiveness of which has been widely proven for different traffic control applications [9].

A further characteristic of this work is that a two-class macroscopic traffic model and a two-class controller are considered, i.e. two classes of vehicles (cars and trucks) are explicitly modelled and the control scheme is designed in order to define specific control actions for each vehicle class. First of all, the use of a two-class traffic model allows to represent the system behaviour more accurately than with a one-class macroscopic model that considers the whole traffic as a homogeneous fluid. Moreover, from the point of view of control, it is possible to devise separate control actions for the two vehicle classes, for instance by differently weighing the presence of cars and trucks in the freeway system; in practice, this calls for separate on-ramp lanes and

signals for cars and trucks, something that is anyhow routinely practiced in some countries (e.g. in The Netherlands and in Australia). Some multi-class models can be found in the literature, such as for instance in [29] introducing a gas-kinetic traffic flow model using a platoon-based multi-class description of traffic flows, and in [30] where the LWR model is extended to include heterogeneous drivers. A more recent multi-class model is FASTLANE, a first order traffic model which considers state-dependent passenger car equivalents [31]. Moreover, some Model Predictive Control approaches for multi-class ramp metering can be found in [32, 33, 34]. The two-class model presented in this paper extends the model proposed in [35], which was based on the macroscopic traffic flow model METANET.

This paper is organized as follows. Section 2 introduces the modeling framework, i.e. describes the two-class traffic model, the emission model and the performance indicators used in the paper. Section 3 is devoted to the optimal control problem formulation, whereas Section 4 describes the numerical solution algorithm adopted in this work. Then, in Section 5 some simulation results are reported and discussed, and the conclusions are drawn in Section 6.

2. The modeling framework

This section reports, first of all, the two-class macroscopic traffic flow model adopted for representing the freeway dynamic behaviour, then, the average-speed emission model considered in the paper and, finally, some performance indicators which are considered of particular interest for this work. Some of these indicators are used in the subsequent definition of the proposed control scheme.

2.1. The two-class traffic model

The considered two-class macroscopic traffic flow model is based on the division of the freeway stretch in N sections and the discretization of the time horizon in K time steps. In the following, $k = 0, \ldots, K$ denotes the temporal stage, $i = 1, \ldots, N$ indicates the section of the freeway stretch, and $c = 1, 2$ represents the vehicle class ($c = 1$ represents the class of cars whereas $c = 2$ indicates the class of trucks). Moreover, let T indicate the sample time interval and L_i the length of section i.

The main aggregate variables of the considered model are specifically defined for each class of vehicles, as listed in the following (see also Fig. 1):

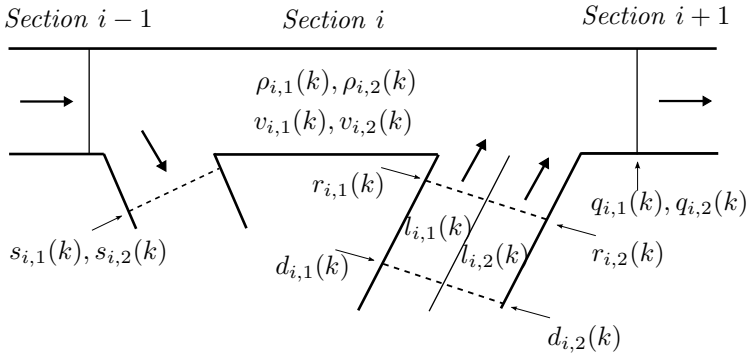

Figure 1: The model variables for a generic freeway section i at a generic time step k.

- $\rho_{i,c}(k)$ is the traffic density of class c in section i at time kT (expressed in vehicles of class c per kilometre);
- $v_{i,c}(k)$ is the mean traffic speed of class c in section i at time kT (expressed in kilometre per hour);
- $q_{i,c}(k)$ is the traffic volume of class c leaving section i during time interval $[kT, (k+1)T)$ (expressed in vehicles of class c per hour);
- $l_{i,c}(k)$ is the queue length of vehicles of class c waiting on the on-ramp of section i at time kT (expressed in vehicles of class c);
- $d_{i,c}(k)$ is the traffic volume of class c requiring to access section i from the on-ramp during time interval $[kT, (k+1)T)$ (expressed in vehicles of class c per hour);
- $r_{i,c}(k)$ is the on-ramp traffic volume of class c entering section i during time interval $[kT, (k+1)T)$ (expressed in vehicles of class c per hour);
- $s_{i,c}(k)$ is the off-ramp traffic volume of class c exiting section i during time interval $[kT, (k+1)T)$ (expressed in vehicles of class c per hour).

In case a certain section i is not provided with on-ramps and off-ramps, the corresponding variables $r_{i,c}(k)$, $s_{i,c}(k)$, $l_{i,c}(k)$ and $d_{i,c}(k)$, $k = 0, \ldots, K-1$, $c = 1, 2$, are fixed equal to 0. To correctly define the two-class model, some variables referred to the total flow of vehicles are also required, as follows:

- $\rho_i(k)$ is the total traffic density in section i at time kT (expressed in cars per kilometre);

- $r_i(k)$ is the total on-ramp traffic volume entering section i during time interval $[kT, (k+1)T)$ (expressed in cars per hour).

The considered model includes some traffic parameters. Specifically, $v_{i,c}^{\mathrm{f}}$ is the free-flow speed referred to class $c = 1, 2$ and section $i = 1, \ldots, N$ (expressed in kilometre per hour), ρ_i^{cr} is the critical density of section $i = 1, \ldots, N$ (expressed in cars per kilometre), $\rho_i^{\max}$ is the jam density of section $i = 1, \ldots, N$ (expressed in cars per kilometre), $r_{i,c}^{\max}$ is the on-ramp capacity for class $c = 1, 2$ and section $i = 1, \ldots, N$ (expressed in vehicles of class c per hour). The choice of expressing the quantities $\rho_i(k)$, $r_i(k)$, ρ_i^{cr} and $\rho_i^{\max}$ in terms of cars is not mandatory (i.e. the same quantities could have been referred to trucks alternatively) but is the most common in the literature.

Moreover, the parameter ς is a conversion factor between cars and trucks. Its meaning is analogous to the definition of passenger car equivalents (PCE), that are considered as the number of passenger cars displaced by a single heavy vehicle of a particular type under prevailing roadway, traffic and control conditions [36]. The factor ς depends on the considered freeway portion and the traffic conditions present in it, as discussed for instance in [37]. In this work a constant factor ς is considered, assuming that it has been suitably estimated on the basis of real data.

The two-class traffic model is given by the following dynamic equations

$$\rho_{i,c}(k+1) = \rho_{i,c}(k) + \frac{T}{L_i}\Big[q_{i-1,c}(k) - q_{i,c}(k) + r_{i,c}(k) - s_{i,c}(k)\Big] \qquad c = 1, 2, \quad i = 1, \ldots, N, \quad k = 0, \ldots, K-1 \quad (1)$$

$$v_{i,c}(k+1) = v_{i,c}(k) + \frac{T}{\tau_c}\Big[V_{i,c}(k) - v_{i,c}(k)\Big] + \frac{T}{L_i} v_{i,c}(k)\big(v_{i-1,c}(k) - v_{i,c}(k)\big) - \frac{\nu_c T\big(\rho_{i+1}(k) - \rho_i(k)\big)}{\tau_c L_i\big(\rho_i(k) + \chi_c\big)} - \delta_c^{\mathrm{on}} T \frac{v_{i,c}(k) r_i(k)}{L_i(\rho_i(k) + \chi_c)} \qquad c = 1, 2, \quad i = 1, \ldots, N, \quad k = 0, \ldots, K-1 \quad (2)$$

$$l_{i,c}(k+1) = l_{i,c}(k) + T\big[d_{i,c}(k) - r_{i,c}(k)\big] \qquad c = 1, 2, \quad i = 1, \ldots, N, \quad k = 0, \ldots, K-1 \quad (3)$$

where τ_c, ν_c, χ_c, δ_c^{on}, $c = 1, 2$, are suitable parameters which in general can be related to each vehicle class. In a real application, these parameters have to be properly tuned with specific identification procedures.

The traffic flow in (1) is obtained as

$$q_{i,c}(k) = \rho_{i,c}(k) \cdot v_{i,c}(k) \qquad c = 1, 2, \quad i = 1, \ldots, N, \quad k = 0, \ldots, K-1 \quad (4)$$

whereas the total density and the total on-ramp traffic volume used in (2) can be computed respectively as

$$\rho_i(k) = \rho_{i,1}(k) + \varsigma \rho_{i,2}(k) \qquad i = 1, \ldots, N, \quad k = 0, \ldots, K-1 \quad (5)$$

$$r_i(k) = r_{i,1}(k) + \varsigma r_{i,2}(k) \qquad i = 1, \ldots, N, \quad k = 0, \ldots, K-1 \quad (6)$$

The steady-state speed density relation $V_{i,c}(k)$ in (2) can be expressed as:

$$V_{i,c}(k) = v_{i,c}^{\text{f}} \cdot \left[1 - \left(\frac{\rho_i(k)}{\rho_i^{\max}} \right)^{l_c} \right]^{m_c} \qquad c = 1, 2, \quad i = 1, \ldots, N, \quad k = 0, \ldots, K-1 \quad (7)$$

where l_c, m_c, $c = 1, 2$, are other model parameters specific for each vehicle class. It is important to note that the steady-state speed density relation for class c depends on the overall traffic density.

If the freeway system is controlled, the on-ramp entering flow $r_{i,c}(k)$ is a portion $\mu_{i,c}(k)$ of the flow $\bar{r}_{i,c}(k)$ that would enter the mainstream if the ramp were not controlled. Therefore $\mu_{i,c}(k) \in [\mu_{i,c}^{min}, 1]$ is the metering rate for the on-ramp of section i at time kT for class c, and when $\mu_{i,c}(k)$ is set equal to 1 no ramp metering is applied. Then, the following relations hold:

$$r_{i,c}(k) = \mu_{i,c}(k) \cdot \bar{r}_{i,c}(k) \qquad c = 1, 2, \quad i = 1, \ldots, N, \quad k = 0, \ldots, K-1 \quad (8)$$

$$\bar{r}_{i,c}(k) = \min \left\{ d_{i,c}(k) + \frac{l_{i,c}(k)}{T}, r_{i,c}^{\max}, r_{i,c}^{\max} \cdot \frac{\rho_i^{\max} - \rho_i(k)}{\rho_i^{\max} - \rho_i^{\text{cr}}} \right\} \qquad c = 1, 2, \quad i = 1, \ldots, N, \quad k = 0, \ldots, K-1 \quad (9)$$

2.2. The average-speed emission model

The average-speed emission models are based on the assumption that the average emissions for a certain pollutant and for a certain type of vehicle only depend on the average speed during a trip. Since analysing the emission models that characterize all the possible typologies of vehicles is out of the scope of this work, in this paper we consider a simplified traffic composition. In particular, as regards the first class of vehicles, we only consider gasoline cars, split in four legislation emission categories (from Euro 1 to Euro 4). For the second class of vehicles, we consider only the case of roads with no slope and half loaded trucks. In case more complex traffic compositions were taken into account, the methodology proposed in this paper could be easily extended.

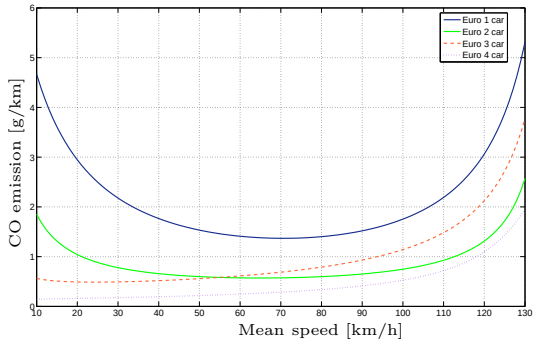

(a)

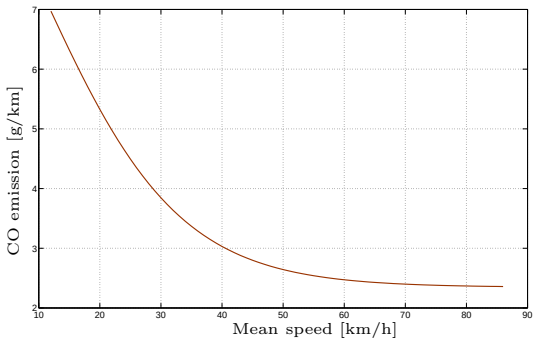

(b)

Figure 2: CO emissions for a car (2a) and for a truck (2b).

Let us start from the first class of vehicles, i.e. cars. Relying on the

COPERT model proposed in [26], the hot emissions for a gasoline passenger car of legislation emission category j are calculated as a function of the mean speed v, with v between 10 and 130 [km/h], i.e.

$$\Xi_1^j(v) = \frac{a_1^j + e_1^j v + f_1^j v^2}{1 + b_1^j v + d_1^j v^2} \tag{10}$$

where a_1^j, b_1^j, d_1^j, e_1^j and f_1^j, $j = 1, \ldots, 4$, are parameters assuming specific values depending on the pollutant under study.

The COPERT model [26] for trucks, in case of roads with no slope and half loaded vehicles, is the following

$$\Xi_2(v) = a_2 + \frac{b_2}{1 + exp(-c_2 + d_2 \ln(v) + e_2 v)} \tag{11}$$

where a_2, b_2, c_2, d_2 and e_2 are specific parameters and (11) is defined for values of the mean speed v between 12 and 86 [km/h].

Fig. 2 shows the curves of CO emissions depending on the mean speed, respectively according to (10) and (11), with the values of the parameters reported in [26].

2.3. Performance indicators

The aim of this work is to control a freeway stretch via ramp metering in order to reduce both congestion and total traffic emissions. It is then useful to introduce some indicators which take into account these aspects.

Let us start from the indicators of traffic emissions. First of all, the emissions in the mainstream (referred to the entire time horizon and the whole freeway stretch), denoted as ME, can be computed by adopting the average-speed models referred to one single vehicle, multiplied by the number of vehicles, as

$$ME = \sum_{k=0}^{K-1} \sum_{i=1}^{N} \left[\sum_{j=1}^{4} L_i \cdot \rho_{i,1}(k) \cdot \gamma_1^j \cdot \Xi_1^j\big(v_{i,1}(k)\big) \right] + \left[L_i \cdot \rho_{i,2}(k) \cdot \Xi_2\big(v_{i,2}(k)\big) \right] \tag{12}$$

The first term in (12) considers the average-speed model (10) referred to one single car of category j, multiplied by the number of these cars, where γ_1^j represents the composition rate of cars of legislation emission j. Obviously, these composition rates must be such that $\sum_{j=1}^{4} \gamma_1^j = 1$. The second term in (12) considers the average-speed model (11) referred to one single truck, multiplied by the number of trucks.

The emissions in the on-ramp (referred to the entire time horizon and the whole freeway stretch), denoted as RE, are computed as

$$RE = \sum_{k=0}^{K-1} \sum_{i=1}^{N} \left[\sum_{j=1}^{4} \gamma_1^j \cdot \alpha_1^j \cdot l_{i,1}(k) \right] + \left[\alpha_2 \cdot l_{i,2}(k) \right] \tag{13}$$

where α_1^j, $j = 1, \ldots, 4$, are constant emission factors obtained from (10) in case of minimum average speed $v = 10$ [km/h]. Analogously, α_2 is obtained from (11) with $v = 12$ [km/h].

Finally, the Total Emissions TE in the freeway can be computed as

$$TE = ME + RE \tag{14}$$

Besides the emissions in the freeway, other important indexes regard the capability of the control scheme to reduce congestion. In the following, some very common performance indexes adopted in the literature (see for instance [38]) are described, properly adapted to the two-class case. First of all, the Total Time Spent (TTS) can be seen as the sum of the Total Travel Time (TTT) and the Total Waiting Time (TWT) and is computed as

$$\begin{aligned} TTS &= TTT + TWT \\ &= \sum_{k=0}^{K-1} \sum_{i=1}^{N} TL_i \left[\rho_{i,1}(k) + \varsigma \cdot \rho_{i,2}(k) \right] + \sum_{k=0}^{K-1} \sum_{i=1}^{N} T \left[l_{i,1}(k) + \varsigma \cdot l_{i,2}(k) \right] \end{aligned} \tag{15}$$

where the traffic density and the queue length for trucks are reported in terms of cars thanks to parameter ς. Hence, the TTS is measured in [cars·hour].

The Total Travelled Distance (TTD), measured in [cars·km], is given by

$$TTD = \sum_{k=0}^{K-1} \sum_{i=1}^{N} \left[L_i \cdot T \left(q_{i,1}(k) + \varsigma \cdot q_{i,2}(k) \right) \right] \tag{16}$$

where, analogously, the traffic volume of trucks is converted in terms of cars by means of ς.

3. Problem formulation

As already mentioned, the objective of the present work is to define a coordinated ramp metering strategy aimed at the reduction of traffic congestion in the freeway and, at the same time, at the minimization of the total

emissions of cars and trucks (both in the mainstream and at the on-ramps). The control strategy is here sought by defining and solving an optimal control problem which turns out to be a finite horizon nonlinear optimal control problem with constrained control variables. An algorithm for obtaining the numerical solution of the proposed problem is described in the following section.

Consider the following discrete-time dynamic system

$$\underline{x}(k+1) = \underline{f}\big[\underline{x}(k), \underline{u}(k)\big] \tag{17}$$

where $\underline{x}(k) \in \mathbb{R}^{\mathrm{n}}, k \in \mathbb{N}$, is the system state and with $\underline{x}(0) = \underline{x}_0$. The system state depends on the system dynamics and on the input control variables $\underline{u}(k) \in \mathbb{R}^{\mathrm{m}}, k \in \mathbb{N}$.

The general formulation of the optimization problem over a finite horizon of K time steps is the following.

Problem 1. *Given the system initial conditions $\underline{x}(0) = \underline{x}_0$, find the control sequence $\underline{u}(k), k = 0, \ldots, K-1$, that minimizes*

$$J = \vartheta[\underline{x}(K)] + \sum_{k=0}^{K-1} \varphi\big[\underline{x}(k), \underline{u}(k)\big] \tag{18}$$

subject to (17) *and*

$$\underline{u}^{min} \leq \underline{u}(k) \leq \underline{u}^{max} \qquad k = 0, \ldots, K-1 \tag{19}$$

In (18) $\vartheta[\cdot]$ represents the final cost while $\varphi[\cdot]$ is the stage cost. The general formulation of Problem 1 is applied to freeway traffic control in the following way. On the basis of the two-class model defined in Section 2.1, it may be observed that by substituting (4) into (1), (5), (6), (7) into (2), and (8), (9) into (3), the two-class traffic flow model equations can be expressed by the general discrete-time model (17). The state vector $\underline{x}(k)$, $k = 0, \ldots, K-1$, consists of the densities $\rho_{i,c}(k)$, the mean speeds $v_{i,c}(k)$, and the queues $l_{i,c}(k)$ for every section $i = 1, \ldots, N$ and for each class $c = 1, 2$. The control vector $\underline{u}(k)$, $k = 0, \ldots, K-1$, corresponds to the ramp metering rates $\mu_{i,c}(k)$, $i = 1, \ldots, N$, $c = 1, 2$.

Moreover, in accordance with the purposes of the considered approach, the chosen objective function is defined as follows

$$J = \beta \cdot \Gamma \cdot TE + (1-\beta) \cdot TTS + \sum_{k=1}^{K-1} \sum_{i=1}^{N} \sum_{c=1}^{2} w_{i,c}^{\mu} \cdot \left[\mu_{i,c}(k) - \mu_{i,c}(k-1)\right]^2 + \sum_{k=0}^{K-1} \sum_{i=1}^{N} \sum_{c=1}^{2} w_{i,c}^{l} \cdot \psi_c\left[l_{i,c}(k)\right]^2 \tag{20}$$

with

$$\psi_c\left[l_{i,c}(k)\right] = max\left\{0, l_{i,c}(k) - l_{i,c}^{max}\right\} \qquad c = 1,2, \quad i,\ldots,N, \quad k = 0,\ldots,K-1 \tag{21}$$

$$\mu_{i,c}^{\min} \leq \mu_{i,c}(k) \leq 1 \qquad c = 1,2, \quad i,\ldots,N, \quad k = 0,\ldots,K-1 \tag{22}$$

The first two terms in cost function (20) are the Total Emissions and the Total Time Spent, given respectively by (14) and (15). In (20) Γ is a coefficient used to make these two terms (TTS and TE) of the same order of magnitude, whereas $\beta \in [0,1]$ is used to properly weigh these two cost terms. The third term in (20), with the weights $w_{i,c}^{\mu}$, $i = 1,\ldots,N$, $c = 1,2$, is introduced in order to prevent oscillations of the control trajectories, whereas the last cost term, with weights $w_{i,c}^{l}$, $i = 1,\ldots,N$, $c = 1,2$, is included to limit the queue lengths at on-ramps.

4. Numerical solution algorithm

As already addressed in the previous section, Problem 1 is a constrained nonlinear optimal control problem. Such problems have appeared in various forms within the freeway traffic control domain, see [6] for an overview. Their numerical solution may be attempted by direct use of available Nonlinear Programming codes, but, given the problem dimensions and complexity, this approach is likely to present unsurmountable difficulties in the case of large freeway infrastructures. A much more efficient numerical solution is obtained by use of the feasible direction algorithm which is adopted within the optimal freeway traffic control tool AMOC [8] and leads to low computation times even for very large-scale freeway traffic control problems, see, e.g. [7, 11]. A version of this algorithm is therefore adopted for the present problem.

The feasible direction algorithm produces the control actions $\underline{u}(k), k = 0, \ldots, K-1$, and the state trajectories $\underline{x}(k)$, $k = 1, \ldots, K$, over the whole time horizon. The algorithm is first of all based on the fulfilment of the necessary optimality conditions. These conditions are expressed in terms of the discrete-time Hamiltonian function that is defined as follows

$$H\big[\underline{x}(k), \underline{u}(k), \underline{\lambda}(k+1)\big] = J\big[\underline{x}(k), \underline{u}(k)\big] + \underline{\lambda}(k+1)^T \cdot \underline{f}\big[\underline{x}(k), \underline{u}(k)\big] \quad (23)$$

where the vector $\underline{\lambda}(\cdot)$ is calculated via backward integration by using the following

$$\underline{\lambda}(k) = \frac{\partial H}{\partial \underline{x}(k)} = \frac{\partial J\big[\underline{x}(k), \underline{u}(k)\big]}{\partial \underline{x}(k)} + \left(\frac{\partial \underline{f}\big[\underline{x}(k), \underline{u}(k)\big]}{\partial \underline{x}(k)}\right)^T \cdot \underline{\lambda}(k+1) \qquad k = 0, \ldots, K-1 \quad (24)$$

starting from the final condition

$$\underline{\lambda}(K) = \frac{\partial \vartheta\big[\underline{x}(K)\big]}{\partial \underline{x}(K)} \quad (25)$$

The optimality conditions that have to be satisfied are (17), (19), (24), (25). For a given control sequence $\underline{u}(k)$, $k = 0, \ldots, K-1$, and for a given initial condition, the state trajectory $\underline{x}(k+1)$ can be found by applying (17), so that the cost criterion only depends on the control variables $\underline{u}(k)$ that can be considered as the independent optimization variables. Thus, the cost criterion can be expressed as $\bar{J}[\underline{u}(k)]$, and the reduced gradient $\underline{g}(k)$ is given by

$$\underline{g}(k) = \frac{\partial H}{\partial \underline{u}(k)} = \frac{\partial \bar{J}[\underline{u}(k)]}{\partial \underline{u}(k)} + \left(\frac{\partial \underline{f}\big[\underline{x}(k), \underline{u}(k)\big]}{\partial \underline{u}(k)}\right)^T \cdot \underline{\lambda}(k+1) \quad (26)$$

Moreover, a saturation vector function $sat(\pi)$ is defined as

$$sat(\pi) = \begin{cases} \pi_{max}, & \text{if } \pi > \pi_{max} \\ \pi_{min}, & \text{if } \pi < \pi_{min} \\ \pi, & \text{else} \end{cases} \quad (27)$$

The adopted numerical algorithm, i.e. the feasible direction algorithm, is widely known in the literature (for more details refer to [39]). In this work a

specific version of this algorithm is used, that is the derivative backpropagation method RPROP, in the version proposed in [9] (the original form of the same algorithm is proposed in [40]). The phases of the adopted algorithm follow.

Phase 1 Guess a feasible initial control sequence $\underline{u}^{(0)}(k)$, $k = 0, \ldots K-1$, and set the iteration index $\imath = 0$.

Phase 2 For each iteration $\imath$, using $\underline{u}^{(\imath)}(k)$ and the initial conditions $\underline{x}(0)$, apply (17) to calculate $\underline{x}^{(\imath)}(k+1)$; then, using $\underline{x}^{(\imath)}(k+1)$ and $\underline{u}^{(\imath)}(k)$, apply (24) via backward integration from the final state (25) to get $\underline{\lambda}^{(\imath)}(k+1)$.

Phase 3 Use $\underline{x}^{(\imath)}(k+1)$, $\underline{u}^{(\imath)}(k)$ and $\underline{\lambda}^{(\imath)}(k+1)$ to compute the components of the reduced gradient $\underline{g}^{(\imath)}(k)$.

Phase 4 Apply the RPROP method to get a new, improved admissible control sequence $\underline{u}^{(\imath+1)}(k)$ by applying the following relation

$$\underline{u}^{(\imath+1)}(k) = sat\big(\underline{u}^{(\imath)}(k) + \underline{\Delta u}^{(\imath)}(k)\big) \tag{28}$$

Each component $\Delta u_i^{(\imath)}(k)$ of the control variable increment $\underline{\Delta u}^{(\imath)}(k)$ is calculated according to the sign of the gradient component $g_i^{(\imath)}(k)$ and the increment component at the previous iteration $\Delta u_i^{(\imath-1)}(k)$, as follows

$$\Delta u_i^{(\imath)}(k) = \begin{cases} -\text{sign}\big(g_i^{(\imath)}(k)\big) \cdot \eta^+ \cdot \Delta u_i^{(\imath-1)}(k) & \text{if } g_i^{(\imath-1)}(k) \cdot g_i^{(\imath)}(k) > 0 \\ -\text{sign}\big(g_i^{(\imath)}(k)\big) \cdot \eta^- \cdot \Delta u_i^{(\imath-1)}(k) & \text{otherwise} \end{cases} \tag{29}$$

where $0 < \eta^- < 1 < \eta^+$. The algorithm starts with $\underline{\Delta u}^{(0)}(k) = \underline{\Delta}$ verifying (28). For the following iterations, according to (28) and (29), if the gradient component maintains its sign, the corresponding increment $\Delta u_i^{(\imath)}(k)$ is slightly increased, by the factor η^+, in order to accelerate the convergence in that region. On the other hand, if there is a change of sign of the gradient component, this means that the algorithm has jumped over a local minimum and the corresponding increment $\Delta u_i^{(\imath)}(k)$ is decreased by the factor η^-. Nevertheless, at each

iteration the calculated $\underline{\Delta u}^{(\imath)}(k)$ may be restricted in a specific interval $[\underline{\Delta}_{min}, \underline{\Delta}_{max}]$.

Phase 5 If for a given scalar σ the convergence test $|J^{(\imath+1)} - J^{(\imath)}|/J^{(\imath)} < \sigma$ is satisfied, stop; otherwise start a new iteration $\imath = \imath + 1$, and go back to Phase 2.

As it is known, there are several techniques for the identification of the search direction, such as steepest descent, quasi-Newton, conjugate gradient methods (for major details see [39]). However the choice to apply the aforementioned method to our optimization problem is suggested by the effective results obtained by applying the RPROP method for traffic control problems, as reported in [9]. Moreover such application does not require a line-search routine as requested by other algorithms, since the control variable increments are calculated, for each iteration, only on the basis of the sign of the gradient components $g_i^{(\imath)}(k)$.

5. Simulation results

In order to demonstrate the effectiveness of the methodology proposed in this paper, a case study has been considered and the results obtained from the application of different control strategies to two control scenarios of such a case study have been compared. In particular, Scenario 1 corresponds to the case in which no restrictions on the maximum queue lengths at the on-ramps are applied, while in Scenario 2 a limit of 50 cars and 5 trucks is imposed for each on-ramp. For each scenario, the system behaviour in the no-control case will be compared with the one provided by the application of the local controller PI-ALINEA (here adopted in the two-class version presented in [27]), and with the optimal solutions found by using the feasible direction algorithm described in this paper. Three optimal solutions adopting the feasible direction algorithm will be analysed, setting different values of the parameter β; these cases correspond to $\beta = 0$ (i.e., only minimizing TTS), $\beta = 0.5$ (i.e., minimizing both TTS and TE) and $\beta = 1$ (i.e., only minimizing TE).

The considered three-lane freeway stretch is 10 [km] long, is composed of $N = 20$ sections with length L_i, $i = 1, \ldots, 20$, set equal to 500 [m]. This stretch presents two on-ramps, located in sections $i = 14$ and $i = 16$, and one off-ramp, located in section $i = 15$. The sample time $T = 10$ [s] has been

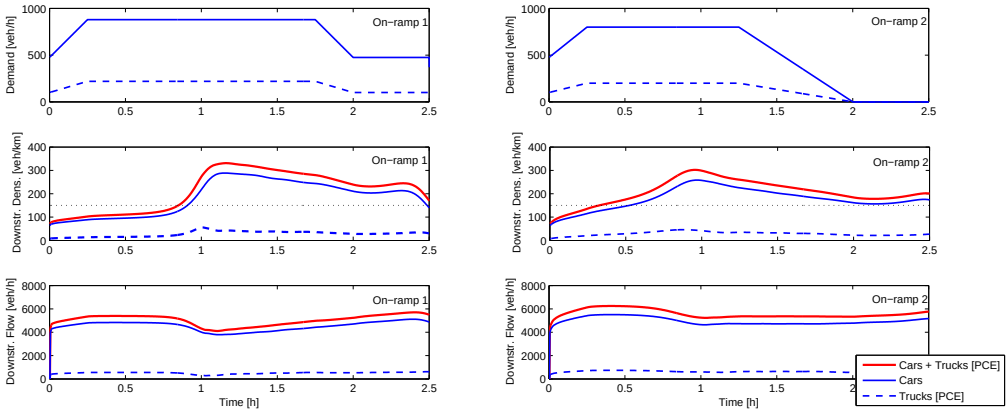

Figure 3: No-control case.

chosen and a total time horizon of two and a half hours (corresponding to $K = 900$) has been used for the simulation tests. The case study is characterized by trapezoidal demand profiles for both vehicle classes, as shown in the upper plots in Fig. 3, whereas the mainstream flow is composed by 3900 [cars/h] and 86 [trucks/h] (344 [PCE/h]). The exit flows from the off-ramps are computed as a percentage, specifically 5%, of the relative mainstream flow.

In order to apply the two-class PI-ALINEA, the set-point value for the density is set equal to the critical density, i.e. 150 [cars/km], while the adopted parameters for the RPROP algorithm are $\eta^+ = 1.2$, $\eta^- = 0.5$, $\Delta_{max} = 0.2$, $\Delta_{min} = 10^{-6}$, $\sigma = 10^{-6}$.

As aforementioned, in Fig. 3 the upper plots indicate the on-ramp demands, whereas the plots in the middle and in the bottom show, respectively, the density and flow evolution downstream the two on-ramps in case the freeway is not controlled. Analysing this figure, it can be noted that the no-control case is characterized by a high congestion in the downstream sections, in which for most of the time the density is much higher than the critical value (indicated in the density plots with a dotted line).

5.1. Scenario 1

Consider first of all Scenario 1, i.e. the case without queue constraints. The system behaviour by applying the two-class PI-ALINEA and the feasible direction algorithm (respectively with $\beta = 0$, $\beta = 0.5$ and $\beta = 1$) are reported in Figs. 4-7. Every figure reports, for each section equipped with on-ramps,

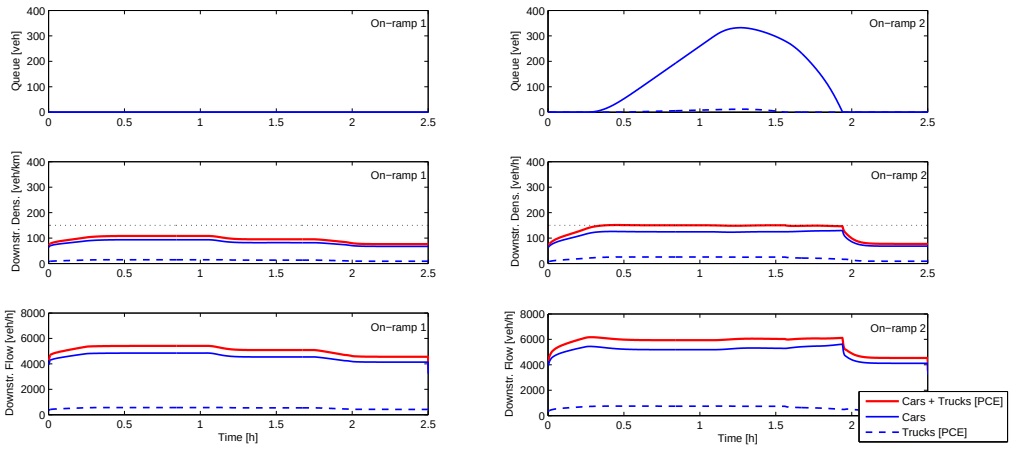

Figure 4: Scenario 1 - Two-class PI-ALINEA.

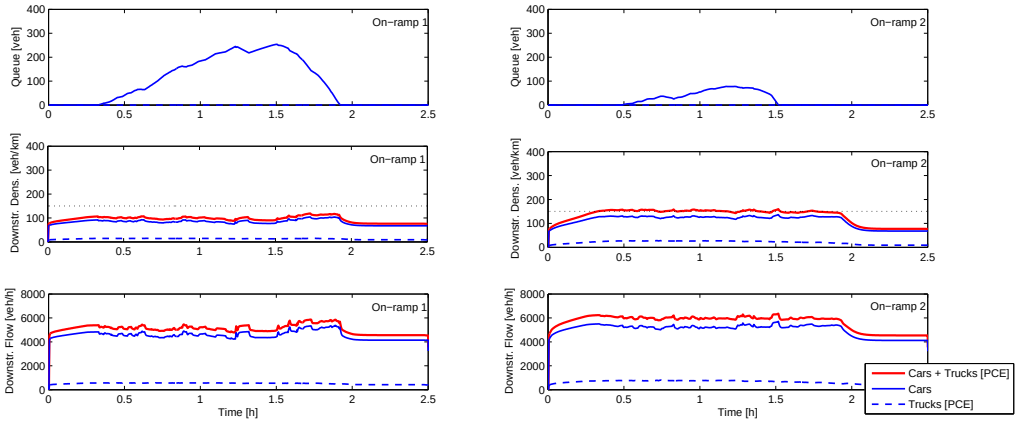

Figure 5: Scenario 1 - Optimal solution with $\beta = 0$.

the queue lengths, the downstream density and the traffic flow. All the controlled cases are characterized by lower densities in comparison with the no-control case and some queues at the on-ramps. Such queues are present in both the on-ramps when the control algorithm is applied, whereas they are present only in the second on-ramp for the system controlled with the

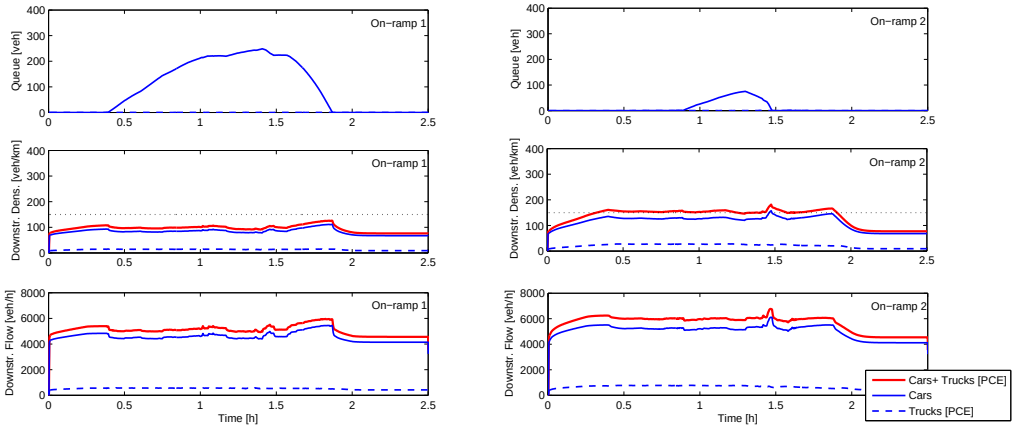

Figure 6: Scenario 1 - Optimal solution with $\beta = 0.5$.

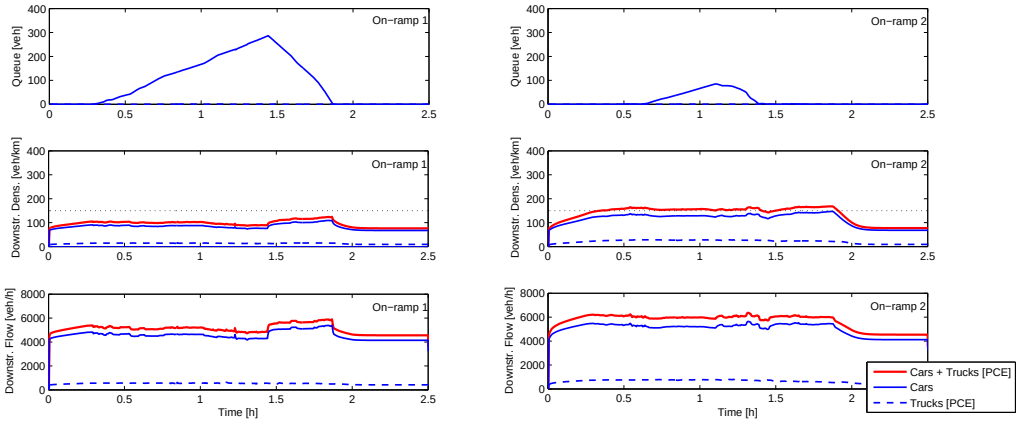

Figure 7: Scenario 1 - Optimal solution with $\beta = 1$.

two-class PI-ALINEA. By varying β in the control algorithm, the system performances do not change significantly. Fig. 8 shows the density evolution in all sections in the considered cases. Again, it is clear that all the controllers are able to reduce congestion phenomena that are instead quite evident in the no-control case.

In Table 1 the different control strategies are compared with the no-

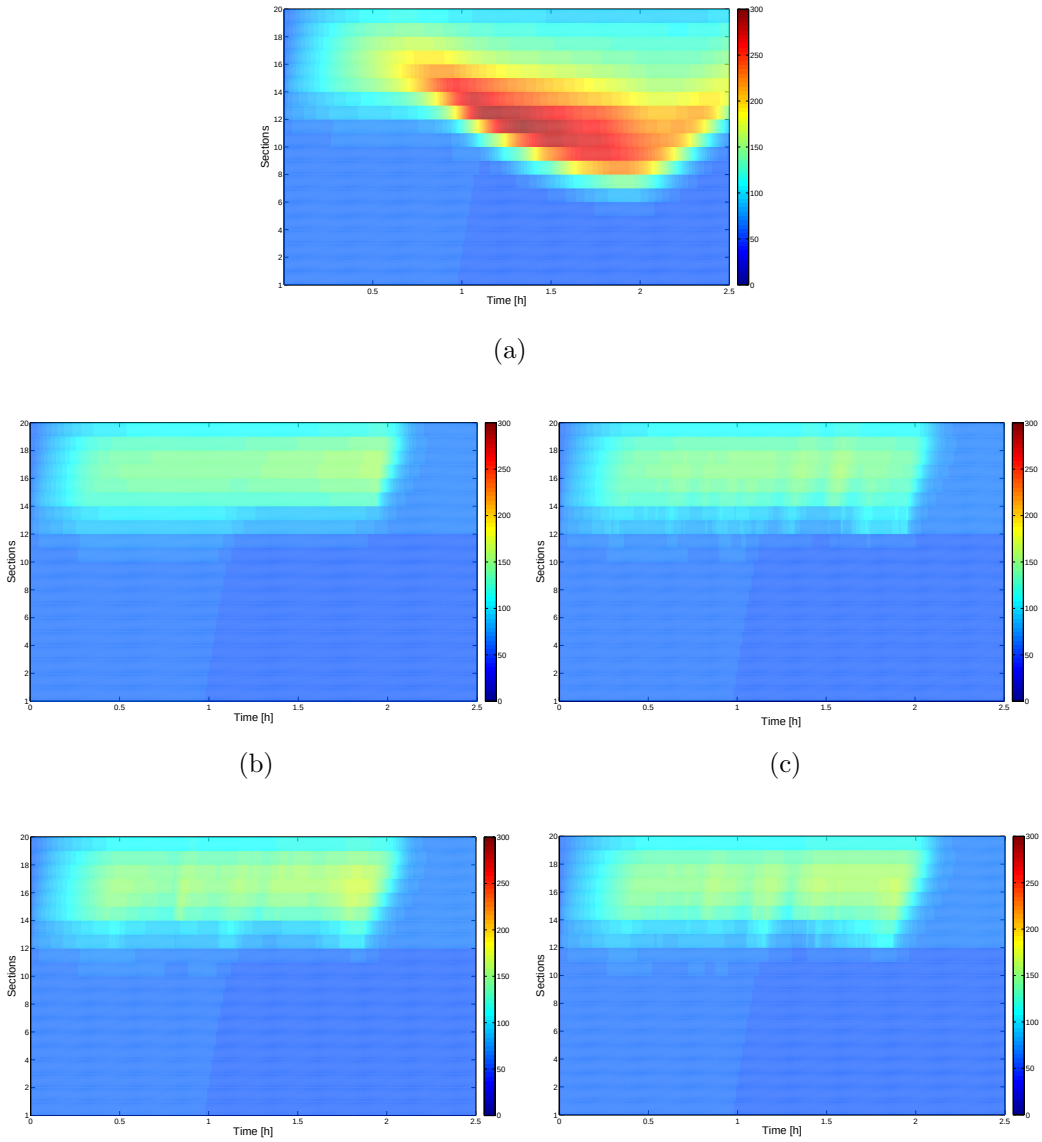

(a)

(b)

(c)

(d)

(e)

Figure 8: Scenario 1 - Mainstream density in the no-control case (8a), with two-class PI-ALINEA (8b), applying the feasible direction algorithm with $\beta = 0$ (8c), $\beta = 0.5$ (8d) and $\beta = 1$ (8e).

control case through some performance indexes. In particular, the considered indexes are the Total Waiting Time TWT, the Total Time Spent TTS,

Table 1: Scenario 1 - Performance indicators.

Control strategy	**TWT** [**veh· h**]	**TTS** [**veh· h**]	**TTS'** [**veh· h**]	**TTS' Red.** [%]	**TE** [**g/km**]	**TE Red.** [%]
No control	0.000	3266.995	3035.577	0.000	1033762.091	0.000
PI-ALINEA	327.058	2610.440	2379.021	21.629	724904.317	29.877
Algorithm $\beta = 0$	284.721	2577.556	2348.112	22.647	705762.085	31.729
Algorithm $\beta = 0.5$	267.458	2577.841	2348.397	22.638	703454.656	31.952
Algorithm $\beta = 1$	264.051	2583.033	2353.589	22.466	705121.848	31.791

the Total Time Spent TTS' computed after the beginning of the congestion (i.e. after about 15 minutes, that is when the congestion starts in the second on-ramp), the TTS' percentage reduction with respect to the no-control case, the Total Emission TE, and the TE percentage reduction with respect to the no-control case. The Total Travelled Distance TTD has been computed and presents similar values for each considered case. The controllers applying the feasible direction algorithm perform better than PI-ALINEA both in terms of Total Time Spent reduction and in terms of Total Emission reduction. By comparing the three cases with $\beta = 0$, $\beta = 0.5$ and $\beta = 1$, it is possible to verify that the system performances are not so different, as already stated by analysing Figs. 5-7. This result is in accordance with the conclusions obtained in [28] where, only analysing the two-class PI-ALINEA controller and considering again the average-speed emission model COPERT, it is concluded that the minimization of emissions and the minimization of congestion in the freeway are not conflicting goals.

All the simulations tests have been realized with a 2.30 GHz Intel(R) Core(TM) i7-3610QM computer with 4 GB RAM with Matlab R2013a software. The computational time requested to solve the three control problems has been of about 120, 410, and 610 [s] for the cases corresponding to $\beta = 0$, $\beta = 1$ and $\beta = 0.5$, respectively.

5.2. Scenario 2

Scenario 2 regards the same freeway stretch but the considered traffic controllers are applied taking into account some limits to the queue lengths at the on-ramps. In particular, the limit of 50 cars and 5 trucks (20 [PCE]) is considered. The evolution in time of the queue lengths, the downstream density and the traffic flow for each section with on-ramps is reported in Figs. 9-12 for the different controllers. As expected, by imposing a limit to the on-ramp queues, such queues are reduced with respect to Scenario 1

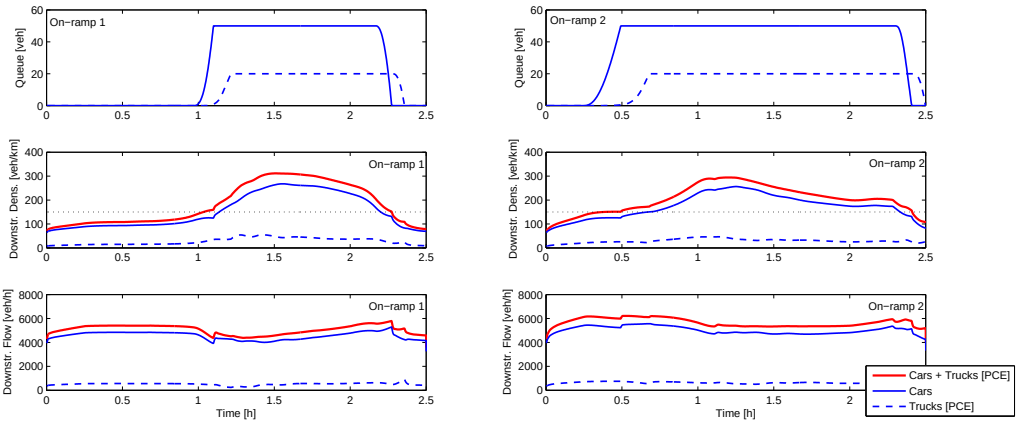

Figure 9: Scenario 2 - Two-class PI-ALINEA.

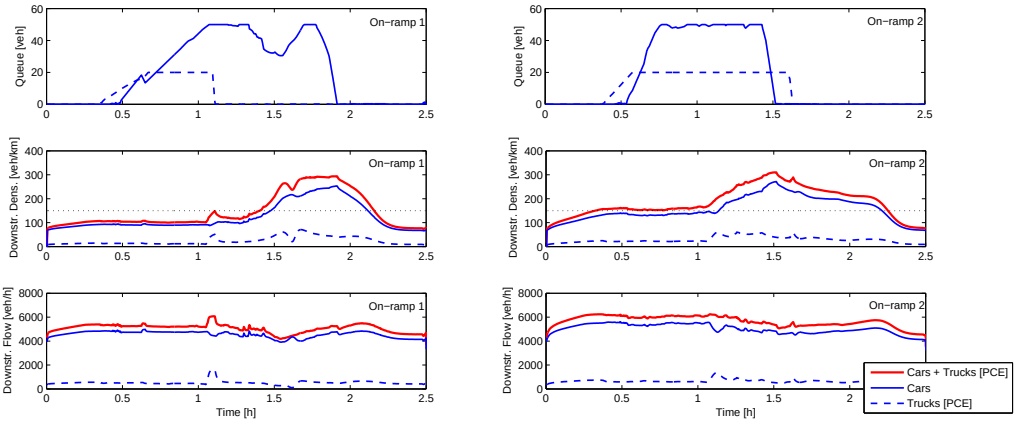

Figure 10: Scenario 2 - Optimal solution with $\beta = 0$.

and, consequently, the density is increased in the section downstream the on-ramp, exceeding for some periods the critical density.

Comparing Fig. 10 (optimal solution with $\beta = 0$, i.e. minimizing the Total Time Spent) with Fig. 12 (optimal solution with $\beta = 1$, i.e. minimizing the Total Emissions), it is quite interesting to see that the evolution of the densities in the sections downstream the on-ramps present similar values

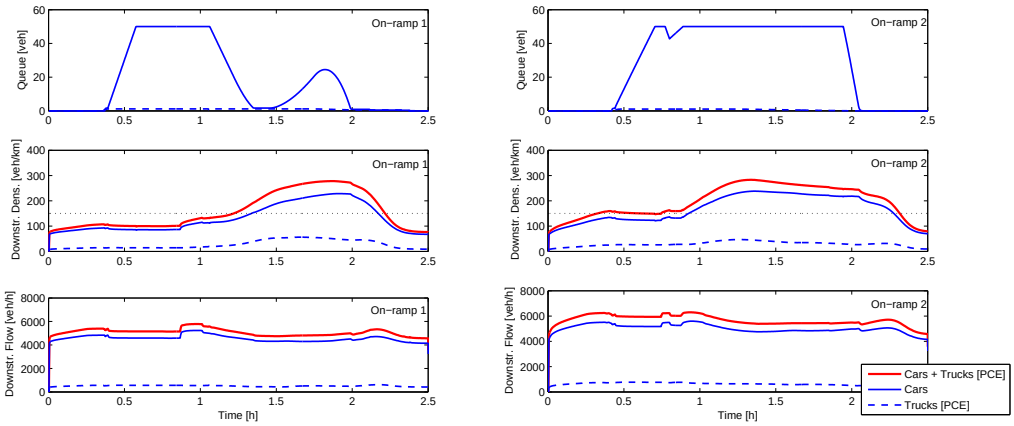

Figure 11: Scenario 2 - Optimal solution with $\beta = 0.5$.

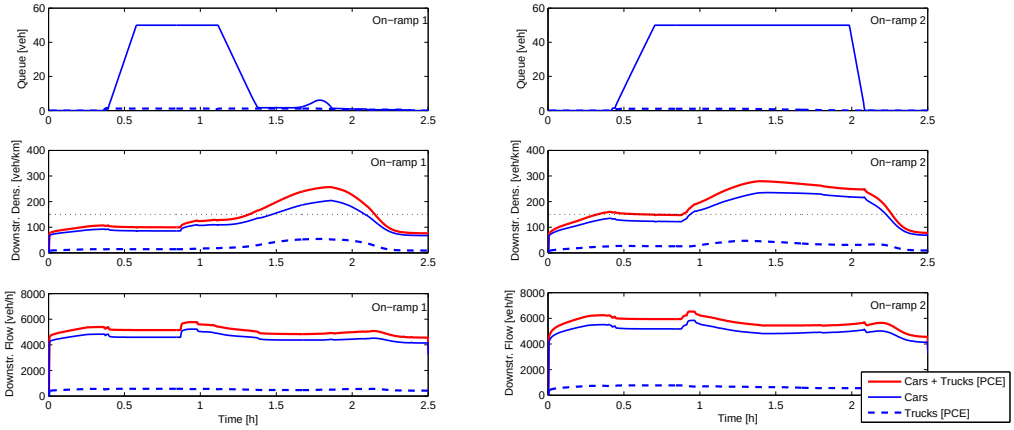

Figure 12: Scenario 2 - Optimal solution with $\beta = 1$.

whereas the on-ramp queue lengths present quite different behaviours. In particular, when the Total Time Spent is minimized ($\beta = 0$), both cars and trucks are queued at the on-ramps, whereas no trucks are present in the on-ramp queues when the Total Emissions are minimized ($\beta = 1$). This is motivated by the fact that, as it is evident in Fig. 2, trucks present high emissions in case of low speeds and, also, their emissions keep decreasing

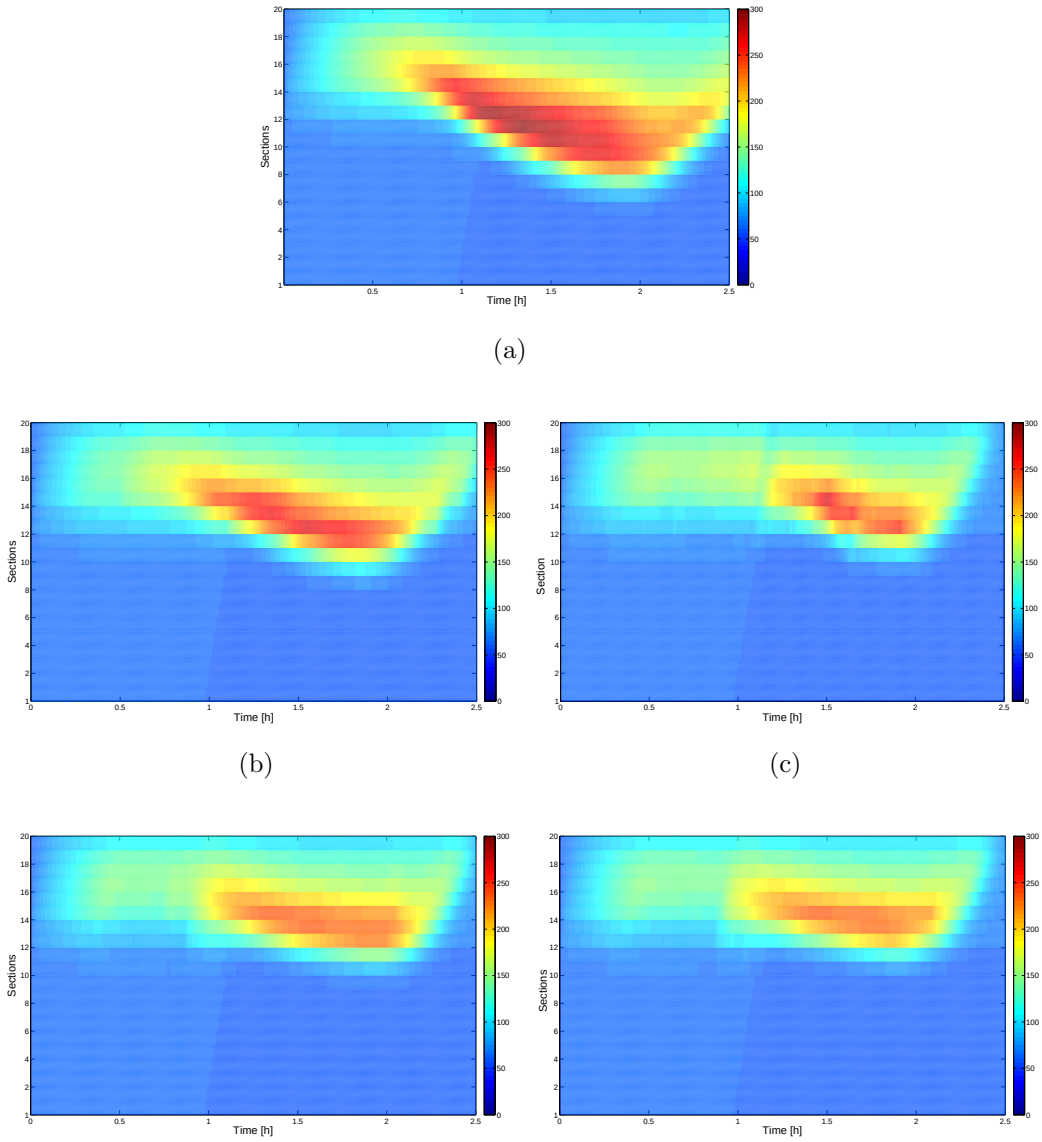

(a)

(b)

(c)

(d)

(e)

Figure 13: Scenario 2 - Mainstream density in the no-control case (13a), with the two-class PI-ALINEA (13b), applying the feasible direction algorithm with $\beta = 0$ (13c), $\beta = 0.5$ (13d) and $\beta = 1$ (13e).

when speed increases. So, if emissions are explicitly minimized, the controller makes trucks enter the freeway without waiting at the on-ramps. The same

considerations can be given analysing the densities in all the freeway for the entire time horizon, as shown in Fig. 13.

Table 2: Scenario 2 - Performance indicators.

Control strategy	**TWT [veh· h]**	**TTS [veh· h]**	**TTS' [veh· h]**	**TTS' Red. [%]**	**TE [g/km]**	**TE Red. [%]**
No control	0.000	3266.995	3035.577	0.000	1033762.091	0.000
PI-ALINEA	217.393	3089.203	2857.784	5.857	943741.071	8.708
Algorithm $\beta = 0$	127.014	2783.742	2554.299	15.855	789240.018	23.654
Algorithm $\beta = 0.5$	117.886	2833.557	2604.114	14.214	806358.052	21.998
Algorithm $\beta = 1$	116.823	2767.310	2537.866	16.396	776091.347	24,925

In Table 2 the different control strategies are compared with the no-control case through the same performance indexes already reported in Table 1 (again, the Total Travelled Distance is similar in the different considered cases). Since in this scenario some constraints on the maximum queue lengths are imposed, the TTS' reductions and the TE reductions are lower than in Scenario 1 but similar conclusions can be drawn. Again, when the control algorithm is applied these reductions are higher than with PI-ALINEA and similar system performances are achieved by varying β between 0 and 1. In all the three cases, the computational time requested to solve the control problem has been equal to 600 [s] approximately.

6. Conclusions

A multi-objective optimal control approach for freeway traffic regulation has been stated and solved in the paper. The two considered control objectives refer to the reduction of traffic congestion situations and to the minimization of traffic emissions. A specific feature of the proposed control scheme is the fact that it explicitly takes into account the presence of two classes of vehicles for which two separate control actions are determined. The overall control problem has been stated as a nonlinear constrained optimal control problem whose solution has been sought by adopting a specific version of the feasible direction algorithm, namely, the derivative backpropagation method RPROP. The effectiveness of the proposed approach has been analyzed and assessed through simulation results in which it is shown that the two parts of the control function are largely non conflicting objectives since both the average travel times and the emissions are reduced if the control actions manage to reduce or eliminate traffic congestion. Having said

that, there are different control options for congestion mitigation, each of which may favour more or less one of both objectives against the other. In such cases, the proposed approach may be appropriately guided to the desired control policy (which reflects a desired trade-off for both objectives) via appropriate selection of the involved weight parameters in the overall objective function. The presented approach may provide an intelligent kernel for flexible real-time control; it may also be used in order to analyse offline potential control scenarios and the related objective trade-offs for specific infrastructures.

Acknowledgments

For the research leading to these results, Prof. Markos Papageorgiou, Prof. Ioannis Papamichail and Dr. Claudio Roncoli have received funding from the European Research Council under the European Union's Seventh Framework Programme (FP/2007-2013) / ERC Grant Agreement n. 321132, project TRAMAN21.

References

[1] M. Papageorgiou, I. Papamichail, Overview of traffic signal operation policies for ramp metering, *Transportation Research Record: Journal of the Transportation Research Board*, vol. 2047, 2008, pp. 28-36.

[2] M. Papageorgiou, H. Hadj-Salem, J.-M. Blosseville, ALINEA: A local feedback control law for on-ramp metering, *Transportation Research Record*, vol. 1320, 1991, pp. 58-64.

[3] M. Papageorgiou, E. Kosmatopoulos, I. Papamichail, Y. Wang, ALINEA maximises motorway throughput - an answer to flawed criticism, *TEC Magazine*, 2007, pp. 271-276.

[4] Y. Wang, M. Papageorgiou, J. Gaffney, I. Papamichail, J. Guo, Local ramp metering in the presence of random-location bottlenecks downstream of a metered on-ramp, *Proc. of 13th IEEE Conference on Intelligent Transportation Systems*, 2010, pp. 1462-1467.

[5] I. Papamichail, M. Papageorgiou, Traffic-Responsive Linked Ramp-Metering Control, *IEEE Transactions On Intelligent Transportation Systems*, vol. 9, 2008, pp. 111-121.

[6] A. Kotsialos, M. Papageorgiou, Motorway network traffic control systems, *European Journal of Operational Research*, vol. 152, 2004, pp. 321-333.

[7] A. Kotsialos, M. Papageorgiou, M. Mangeas, H. Haj-Salem, Coordinated and integrated control of motorway networks via non-linear optimal control, *Transportation Research Part C*, vol. 10, 2002, pp. 65-84.

[8] A. Kotsialos, M. Papageorgiou, F. Middelham, Optimal coordinated ramp metering with AMOC, *Transportation Research Record*, vol. 1748, 2001, pp. 55-65.

[9] M. Papageorgiou, A. Kotsialos, Nonlinear optimal control applied to coordinated ramp metering, *IEEE Transactions on Intelligent Transportation Systems*, vol. 12, 2004, pp. 920-933.

[10] I. Papamichail, A. Kotsialos, I. Margonis, M. Papageorgiou, Coordinated ramp metering for freeway networks A model-predictive hierarchical control approach, *Transportation Research Part C*, vol. 18, 2010, pp. 311-331.

[11] R.C. Carlson, I. Papamichail, M. Papageorgiou, A. Messmer, Optimal mainstream traffic flow control of large-scale motorway networks, *Transportation Research Part C*, vol. 18, 2010, pp. 193-212.

[12] A. Hegyi, B. De Schutter, H. Hellendoorn, Model predictive control for optimal coordination of ramp metering and variable speed limits, *Transportation Research C*, vol. 13, 2005, pp. 185-209.

[13] T. Bellemans, B. De Schutter, B. De Moor, Model predictive control for ramp metering of motorway traffic: A case study, *Control Engineering Practice*, vol. 14, 2006, pp. 757-767.

[14] M. Papageorgiou, J.-M. Blosseville, H. Hadj-Salem, Modelling and real-time control of trafficc flow on the southern part of Boulevard Périphérique in Paris: Part I: Modelling, *Transportation Research A*, vol. 24, 1990, pp. 345-359.

[15] A. Ferrara, A. Nai Oleari, S. Sacone, S. Siri, An event-triggered Model Predictive Control scheme for freeway systems, *Proc. of the 51st IEEE Conference on Decision and Control*, 2012, pp. 6975-6982.

[16] N. Groot, B. De Schutter, S. Zegeye, H. Hellendoorn, Model-based predictive traffic control: A piecewise-affine approach based on METANET, *Proc. of the 18th IFAC World Congress*, 2011, pp. 10709-10714.

[17] L. Maggi, M. Maratea, S. Sacone, S. Siri, Computational analysis of freeway traffic control based on a linearized prediction model, *Proc. of the 52nd IEEE Conference on Decision and Control*, 2013, pp. 886-891.

[18] M. Papageorgiou, A. Kotsialos, Freeway Ramp Metering: An Overview, *IEEE Transactions on Intelligent Transportation Systems*, vol. 3, 2002, pp. 271-281.

[19] A. Csikós, T. Luspay, I. Varga, Modeling and optimal control of travel times and traffic emission on freeways, *Proc. of the 18th IFAC World Congress*, 2011, pp. 13058-13063.

[20] A. Csikós, I. Varga, K.M. Hangos, A simple dynamic model for the dispersion of motorway traffic emission, *Proc. of 16th International IEEE Annual Conference on Intelligent Transportation Systems*, 2013, pp. 1559-1564.

[21] S.K. Zegeye, B. De Schutter, J. Hellendoorn, E.A. Breunesse, A. Hegyi, A predictive traffic controller for sustainable mobility using parameterized control policies, *IEEE Transactions on Intelligent Transportation Systems*, vol. 13, 2012, pp. 1420-1429.

[22] S.K. Zegeye, B. De Schutter, J. Hellendoorn, E.A. Breunesse, A. Hegyi, Integrated macroscopic traffic flow, emission, and fuel consumption model for control purposes, *Transportation Research C*, vol. 31, 2013, pp. 158-171.

[23] J.L. Horowitz, *Air quality analysis for urban transportation planning*, MIP Press, 1982.

[24] T.J. Barlow, P.G. Boulter, *Emissions factors 2009: Report 2 - a review of the average-speed approach for estimating hot exhaust emissions*, TRL, 2009.

[25] L. Ntziachristos, Z. Samaras, Speed-dependent representative emission factors for catalyst passenger cars and influencing parameters, *Atmospheric Environment*, vol. 34, 2000, pp. 4611-4619.

[26] L. Ntziachristos, C. Kouridis, Road transport emission chapter of the EMEP/CORINAIR Emission Inventory Guidebook, *European Environment Agency Technical Report No. 16/2007*, Copenhagen, Denmark, 2007.

[27] C. Pasquale, S. Sacone, S. Siri, Two-class emission traffic control for freeway systems, *Proc. of the 19th IFAC World Congress*, 2014, pp. 936-941.

[28] C. Pasquale, S. Sacone, S. Siri, Ramp metering control for two vehicle classes to reduce traffic emissions in freeway systems, *Proc. of the European Control Conference*, 2014, pp. 2588-2593.

[29] S.P. Hoogendoorn, P.H.L. Bovy, Platoon-Based Multiclass Modeling of Multilane Traffic Flow, *Networks and Spatial Economics*, vol. 1, 2001, pp. 137-166.

[30] G.C.K. Wong, S.C. Wong, A multi-class traffic flow model - an extension of LWR model with heterogeneous drivers, *Transportation Research A*, vol. 36, 2002, pp. 827-841.

[31] J.W.C van Lint, S.P. Hoogendoorn, M. Schreuder, FASTLANE: New Multiclass First-Order Traffic Flow Model, *Transportation Research Record*, vol. 2088, 2008, pp. 177-187.

[32] P. Deo, B. De Schutter, A. Hegyi, Model predictive control for multi-class traffic flows, *Proc. of the 12th IFAC Symposium on Transportation Systems*, 2009, pp. 25-30.

[33] T. Schreiter, H. van Lint, S. Hoogendoorn, Multi-class Ramp Metering: Concepts and Initial Results, *Proc. of 14th International IEEE Conference on Intelligent Transportation Systems*, 2011, pp. 885-889.

[34] S. Liu, B. De Schutter, H. Hellendoorn, Model Predictive Traffic Control Based on a New Multi-Class METANET Model, *Proc. of 19th IFAC World Congress*, 2014, pp. 8781-8786.

[35] C. Caligaris, S. Sacone, S. Siri, Model predictive control for multiclass freeway traffic, *Proc. of the European Control Conference*, 2009, pp. 1764-1769.

[36] *Special Report 209: Highway Capacity Manual*, 3rd Edition, Transportation Research Board, Washington DC, 1994.

[37] A.F. Al-Kaisy, F.L. Hall, E.S. Reisman, Developing passenger car equivalents for heavy vehicles on freeways during queue discharge flow, *Transportation Research A*, vol. 36, 2002, pp. 725-742.

[38] H. Haj-Salem, M. Papageorgiou, Ramp metering impact on urban corridor traffic: Field results, *Transportation Research A*, vol. 29, 1995, pp. 303-319.

[39] M. Papageorgiou, M. Marinaki, A feasible direction algorithm for the numerical solution of optimal control problems, Dynamic Syst. Simulation Lab., Technical University of Crete, Chania, Greece, 1995.

[40] M. Riedmiller, H. Braun, A directive adaptive method for faster backpropagation learning: the RPROP algorithm, *Proc. IEEE International conference Neural Networks*, 1993, pp. 586-591.